Available online at www.sciencedirect.com
SCIENCE DIRECT®
Pattern Recognition 38 (2005) 1791–1798
PATTERN RECOGNITION
THE JOURNAL OF THE PATTERN RECOGNITION SOCIETY
www.elsevier.com/locate/patcog

Coarse iris classification using box-counting to estimate fractal dimensions

Li Yu[a], David Zhang[b,*], Kuanquan Wang[a], Wen Yang[a]

[a] *School of Computer Science and Technology, Harbin Institute of Technology (HIT), Harbin 150001, China*
[b] *Biometric Research Center, Department of Computing, Hong Kong Polytechnic University, Kowloon, Hong Kong*

Received 15 September 2004; received in revised form 17 March 2005; accepted 17 March 2005

Abstract

This paper proposes a novel algorithm for the automatic coarse classification of iris images using a box-counting method to estimate the fractal dimensions of the iris. First, the iris image is segmented into sixteen blocks, eight belonging to an upper group and eight to a lower group. We then calculate the fractal dimension value of these image blocks and take the mean value of the fractal dimension as the upper and the lower group fractal dimensions. Finally, all the iris images are classified into four categories in accordance with the upper and the lower group fractal dimensions. This classification method has been tested and evaluated on 872 iris cases, and the proportions of these categories in our database are 5.50%, 38.54%, 21.79%, and 34.17%. The iris images are classified with two algorithms, the double threshold algorithm, which classifies iris images with an accuracy of 94.61%, and the backpropagation algorithm, which is 93.23% accurate. When we allow for the border effect, the double threshold algorithm is 98.28% accurate.

Keywords: Box counting; Fractal dimension; Iris image; Coarse classification

1. Introduction

Biometrics is one of the most important and reliable methods for computer-aided personal identification, having a wide range of applications in government programs such as national ID cards, in visas and visa processing, and in the war against terrorism, as well as having personal applications in areas such as logical and physical access control. The fingerprint is the most widely used biometric feature [1,2], but the most reliable feature is the iris [3,4] and it is this that accounts for its use in identity management in government departments requiring high security.

The iris contains abundant textural information which is often extracted in current recognition methods. Daugman's method, based on phase analysis, encodes the iris texture pattern into a 256 byte iris code by using some two-dimensional Gabor filters, and taking the Hamming distance [3,4] to match the iris code. Wildes [5] matches images using Laplacian pyramid multi-resolution algorithms and a Fisher classifier. This approach, however, has proven to be computationally expensive and is suitable only for verification. Boles [6] extract iris features using a one-dimensional wavelet transform, but this method has been tested only on a small database. Ma et al. [7] construct a bank of spatial filters whose kernels are suitable for use in iris recognition. They have also developed a preliminary Gaussian–Hermite moments-based method which uses local intensity variations of the iris [8]. They recently proposed an improved method based on characterizing key local variations [9].

* Corresponding author. Tel.: +852 2766 7271; fax: +852 2774 0842.
E-mail address: csdzhang@comp.polyu.edu.hk (D. Zhang).

0031-3203/$30.00
doi:10.1016/j.patcog.2005.03.015

Although all these methods obtain good recognition results, all iris authentication methods require the input iris image to be matched against a large number of iris images in a database. This is very time consuming, especially with the iris databases being used in identity recognition growing ever larger. To reduce both the search time and computational complexity, it would be desirable to be able to classify an iris image before matching, so that the input iris is matched only with the irises in its corresponding category, but as yet, the subject of iris classification has received little attention in the literature.

This paper is intended to contribute to the establishment of meaningful quantitative indexes. One such index can be established by using box-counting analysis to estimate the fractal dimensions of iris images with or without self-similarity. This allows us to classify the iris image into four categories according to their texture and structure.

This paper is organized as follows. Section 2 discusses fractal dimension and the box-counting method. Section 3 describes iris image processing and explains the criteria for iris classification. Section 4 reports our experimental results. Section 5 offers a brief conclusion.

2. Counting boxes to estimate the fractal dimension of the iris

The concept of the fractal was first introduced by Mandelbrot [10], who used it as an indicator of surface roughness. It was later applied by Pentland [11] in natural scene analysis and by Keller et al. [12] in textured image segmentation with the gray level replaced by the fractal dimension. The fractal dimension has been used in image classification to measure surface roughness where different natural scenes such as mountains, clouds, trees, and deserts generate different fractal dimensions. Of the wide variety of methods for estimating the fractal dimension that have so far been proposed [13,14], the box-counting method is one of the more widely used ones [15], as it can be computed automatically and can be applied to patterns with or without self-similarity.

In the box-counting method, an image measuring size $R \times R$ pixels is scaled down to $s \times s$, where $1 < s \leqslant R/2$, and s is an integer. Then $r = s/R$. The image is treated as a three-dimensional space, where two dimensions define the coordinates (x, y) of the pixels and the third coordinate (z) defines their grayscale values. The (x, y) is partitioned into grids measuring $s \times s$. On each grid there is a column of boxes measuring $s \times s \times s$. If the minimum and the maximum grayscale levels in the (i, j)th grid fall into, the kth and lth boxes, respectively, the contribution of n_r in the (i, j)th grid is defined as

$$n_r(i, j) = l - k + 1. \tag{1}$$

In this method N_r is defined as the summation of the contributions from all the grids that are located in a window of the image

$$N_r = \sum_{i,j} n_r(i, j). \tag{2}$$

If N_r is computed for different values of r, then the fractal dimension can be estimated as the slope of the line that best fits the points $(\log(1/r), \log N_r)$.

The complete series of steps for calculating the fractal dimension are as follows. First, the image is divided into regular meshes with a mesh size of r. We then count the number of square boxes that intersect with the image N_r. The number N_r is dependent on the choice of r. We next select several size values and count the corresponding number N_r. Following this, we plot the slope D formed by plotting $\log(N_r)$ against $\log(1/r)$. This indicates the degree of complexity, or the dimensions of the fractal. Finally, a straight line is fitted to the plotted points in the diagram using the least-squares method. In accordance with Mandelbrot's view, the linear regression equation used to estimate the fractal dimension is

$$\log(N_r) = \log(K) + D \log(1/r), \tag{3}$$

where K is a constant and D denotes the dimensions of the fractal set.

3. Iris classification

3.1. Image preprocessing

An iris image has a unique and complex structure made up of numerous minute interlacing characteristics such as freckles, coronas, furrows, stripes, and crypts. Nonetheless, an iris also displays a variety of textures which can be broadly classified. These textures can be represented numerically, as a calculation of the fractal dimension. The calculation of the fractal dimension begins with preprocessing the original image to localize and normalize the iris. A captured iris image is a two-dimensional array $(M \times N)$. The gray level of a point (x, y) is described as $I(x, y)$. After localizing an iris, we detect the inner and outer boundaries. In an eye image, the iris may be partially concealed by the upper eyelid, the lower eyelid, or the eyelash. To exclude these influences, image preprocessing makes use of only the inner $\frac{3}{4}$ of the lower half of an iris. As the size of an iris in a captured image always varies, the detected iris is normalized into a rectangular block using the following mapping:

$$I(x(r, \theta), y(r, \theta)) \rightarrow I(r, \theta), \tag{4}$$

where $x(r, \theta)$ and $y(r, \theta)$ are the linear combinations of a point in the inner boundary $x_{Inner}(\theta), y_{Inner}(\theta))$ and a point in the outer boundary $(x_{Outer}(\theta), y_{Outer}(\theta))$ which are along the same radii:

$$\begin{aligned} x(r, \theta) &= (1 - r)x_{Inner}(\theta) + r x_{Outer}(\theta) \\ y(r, \theta) &= (1 - r)y_{Inner}(\theta) + r y_{Outer}(\theta), \\ & r \in [0, 1] \quad \text{and} \quad \theta \in [0, \pi]. \end{aligned} \tag{5}$$

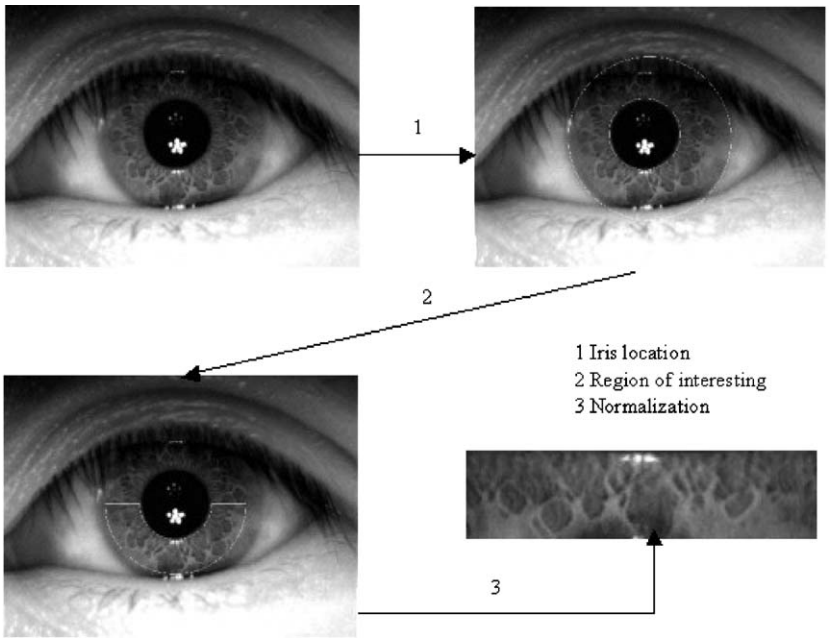

Fig. 1. Preprocessing of iris image.

In our experiments, the preprocessed images were transformed into images measuring 256×64. Fig. 1 illustrates the iris image preprocessing process.

Because all iris images have a similar texture near the pupil, we do not use the upper part of the iris image when classifying an iris. Rather we make use only of the middle and lower part of the iris image. Preliminarily, we use the box-counting method to calculate the fractal dimension. To do this, we first divide a preprocessed iris image into sixteen regions. Eight regions are then drawn from the middle part of the iris image, as shown in Fig. 2. We call these the upper group. The remaining eight regions are drawn from the bottom part of the iris image. These are referred to as the lower group. From these sixteen regions we obtain sixteen 32×32 image blocks. We then use the box-counting method to calculate the fractal dimensions of these image blocks. This produces sixteen fractal dimensions, $FD_i (i = 1, 2, \ldots, 16)$. The mean values of the fractal dimensions of the two groups are taken as the upper and lower group fractal dimensions, respectively.

$$FD_{upper} = \frac{\sum_{i=1}^{8} FD_i}{8},$$

$$FD_{lower} = \frac{\sum_{i=9}^{16} FD_i}{8}. \tag{6}$$

Once we have determined the values of the upper and the lower group fractal dimensions, we can classify the iris image using either the double threshold algorithm or the backpropagation algorithm.

3.2. Classifying an iris using the double threshold algorithm

The double threshold algorithm uses two thresholds to classify the iris into the following four categories, according to the values of the upper and lower group fractal dimensions.

Category 1 (*net structure*). The iris image appears loose and fibrous. The fibers are open and coarse, and there are large gaps in the tissue. The values of both the upper and lower group fractal dimensions are less than the first threshold E_I.

$$\{(FD_{upper}, FD_{lower}) | FD_{upper} < E_I \quad \text{AND} \quad FD_{lower} < E_I\} \tag{7}$$

Fig. 3(a) shows a category 1 iris.

Category 2 (*silky structure*). The iris image appears silky. It displays few fibers and little surface topography. The Autonomic Nerve Wreath (also known as the Ruff and Collarette) is usually located less than one-third the distance from the pupil to the iris border. The values of the upper and lower group fractal dimensions are more than the second threshold E_{II}.

$$\{(FD_{upper}, FD_{lower}) | FD_{upper} > E_{II} \quad \text{AND} \quad FD_{lower} > E_{II}\} \tag{8}$$

Fig. 3(b) shows a category 2 iris.

Category 3 (*linen structure*). The iris image appears to have a texture between those of categories 1 and 2. The Autonomic Nerve Wreath usually appears one-third to halfway

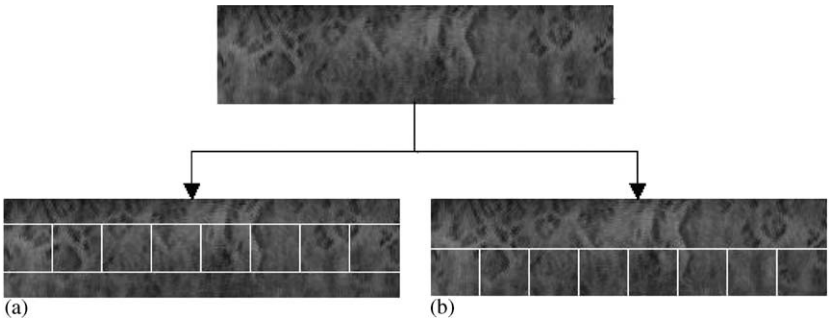

Fig. 2. Image segmentation: (a) upper group and (b) lower group.

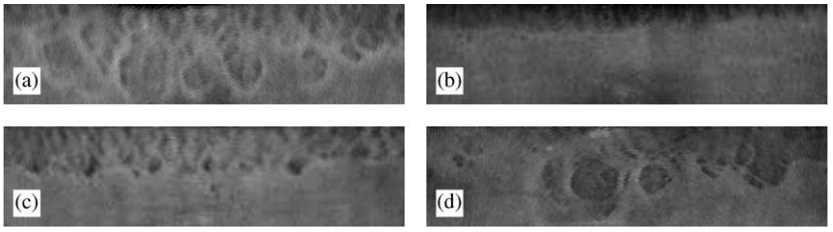

Fig. 3. Examples of each iris category after processing.

between the pupil and the iris border, and the surface of ciliary zone is flat. (The Autonomic Nerve Wreath divides the iris into two zones, an inner pupillary zone, and an outer ciliary zone.) The value of the lower group fractal dimension is more than the second threshold E_{II} and the value of the upper group fractal dimension is less than the second threshold E_{II}.

$$\{(FD_{upper}, FD_{lower})|FD_{upper} < E_{II} \quad \text{AND} \quad FD_{lower} > E_{II}\} \tag{9}$$

Fig. 3(c) shows a category 3 iris.

Category 4 (*hessian structure*). The iris image appears to have a texture similar to category 3 but with a few gaps (lacunae) in the ciliary zone. When the upper and lower group fractal dimension values of an iris fail to satisfy the rules of categories 1, 2, or 3, they are classified into category 4. Fig. 3(d) shows a category 4 iris.

Fig. 3 shows the range of possible textures. categories 3 and 4 are both in a range between categories 1 and 2. Category 3 is more like category 2 and category 4 is more like category 1. Table 1 shows the fractal dimension values of the four categories of the images in Fig. 3.

An input iris is thus categorized by using five steps:

1. Localize the iris boundary and extract the iris image from the eye image.
2. Normalize the iris image into an 256×64 image block.
3. Separate the iris image into sixteen image blocks measuring 32×32 pixels.

Table 1
Iris classification with $E_I = 2.2100$ and $E_{II} = 2.2500$

	Category 1	Category 2	Category 3	Category 4
FD_{upper}	2.1780	2.2648	2.1925	2.2011
FD_{lower}	2.2009	2.2610	2.2556	2.2324

4. Calculate the fractal dimension using the box-counting method and obtain two mean fractal dimension values FD_{upper} and FD_{lower} using formula (6).
5. Compare these two values, FD_{upper} and FD_{lower} with E_I and E_{II}, and then classify the iris image into one of the defined categories using formulae (7), (8) and (9).

Because the value of a fractal dimension is continuous, when classifying, we must take into account the border effect. For the value near the threshold, we cannot simply classify the iris image into one category. Therefore, the nearby categories should be considered at the same time. The complementary rules for classifying the image are as follows:

Rule 1. If $\{(FD_{upper}, FD_{lower})|FD_{upper} \leqslant E_I$ AND $(E_I - \Delta E \leqslant FD_{lower} \leqslant E_I + \Delta E)\}$ or $\{(FD_{upper}, FD_{lower})|(E_I - \Delta E \leqslant FD_{upper} \leqslant E_I + \Delta E)$ AND $FD_{lower} \leqslant E_I\}$, the image belongs to Category 1 or 4, so Categories 1 and 4 should be matched. Here ΔE is a small value.

Rule 2. If $\{(FD_{upper}, FD_{lower})|(E_{II} - \Delta E \leqslant FD_{upper} \leqslant E_{II} + \Delta E)$ AND $E_{II} \leqslant FD_{lower}\}$ or $\{(FD_{upper}, FD_{lower})|E_{II} \leqslant FD_{upper}$ AND $(E_{II} - \Delta E \leqslant FD_{lower} \leqslant E_{II} + \Delta E)\}$, the

image belongs to Category 2 or 3, so Categories 2 and 3 should be matched.

Rule 3. If $\{(FD_{upper}, FD_{lower})|FD_{upper} < E_{II} - \Delta E$ AND $(E_{II} - \Delta E < FD_{lower} < E_{II} + \Delta E)\}$ the image belongs to Category 3 or 4, so Categories 3 and 4 should be matched.

3.3. Classifying an iris using the backpropagation algorithm

The backpropagation algorithm is one of the most popular and widely used network-learning algorithms [16–19]. The input layer consists of two nodes which are the two mean values of the fractal dimensions of the upper and lower groups FD_{upper} and FD_{lower}. The output layer also consists of two nodes. When $y_1 = 0$ and $y_2 = 0$, the output represents category 1; $y_1 = 0$ and $y_2 = 1$, the output represents category 2; $y_1 = 1$ and $y_2 = 0$, the output represents category 3; $y_1 = 1$ and $y_2 = 1$, the output represents category 4. All of the nodes in each layer are fully connected. To achieve high accuracy, the number of training samples must be selected with caution.

4. Experimental results

Extensive experiments on a large image database were carried out to evaluate the effectiveness and accuracy of the proposed methods. The irises were coarsely classified using two algorithms, the double threshold and backpropagation.

An iris image is correctly classified when the label of its category is the same as that of the iris. When there is no such match, the iris has been misclassified. The following subsections detail the experiments and their results.

4.1. The image database

Our iris classification algorithm was tested on a database containing 872 iris images captured from 218 persons having both left and right eyes. There are two images of each eye.

Table 2
Distribution of each category in our database

Category No.	1	2	3	4
Number of iris	48	336	190	298
Percent (%)	5.50	38.54	21.79	34.17

The images measure 758×568 with eight bits per pixel and the irises have been labeled manually. In this database, 48 samples belong to category 1, 336 belong to category 2, 190 belong to category 3 and 298 belong to category 4. Table 2 lists the distribution of each category in our iris database. Samples from the database are shown in Fig. 4. The images in the first column belong to Category 1, the images in the second column belong to Category 3, and so on.

4.2. Results of the classification using the double threshold algorithm

Because the values of E_I and E_{II} are quite important for the result of classification, many experiments have been conducted to select the best values. Figs. 5(a) and (b) depict curves showing accuracy relative to the change of E_I and E_{II}. In Fig. 5(a), let $E_{II} = 2.2500$, the curve shows accuracy relative to the change of E_I. Here the x-axis is the value of E_I and the y-axis is the classification accuracy. The change of E_I can affect the classification accuracy of categories 1 and 4. When $E_I = 2.2100$, the classification is close to the most accurate one. In Fig. 5(b), the curve is the accuracy versus the change of E_{II}. $E_I = 2.2100$. Here the x-axis is the value of E_{II} and y-axis is again the classification accuracy. A change in E_{II} can affect the accuracy of categories 2, 3 and 4. Fig. 5(b) reveals that when $E_{II} = 2.2500$, the classification is the most accurate. So we select $E_I = 2.2100$ and $E_{II} = 2.2500$.

After selecting the values for E_I and E_{II}, we carried out experiments on these two thresholds to classify the iris. Of the 872 irises in the database, 47 samples were misclassified:

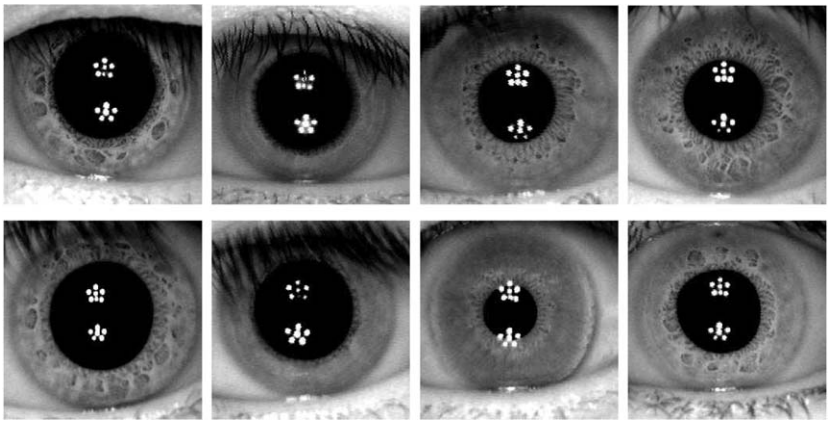

Fig. 4. Iris samples from the database.

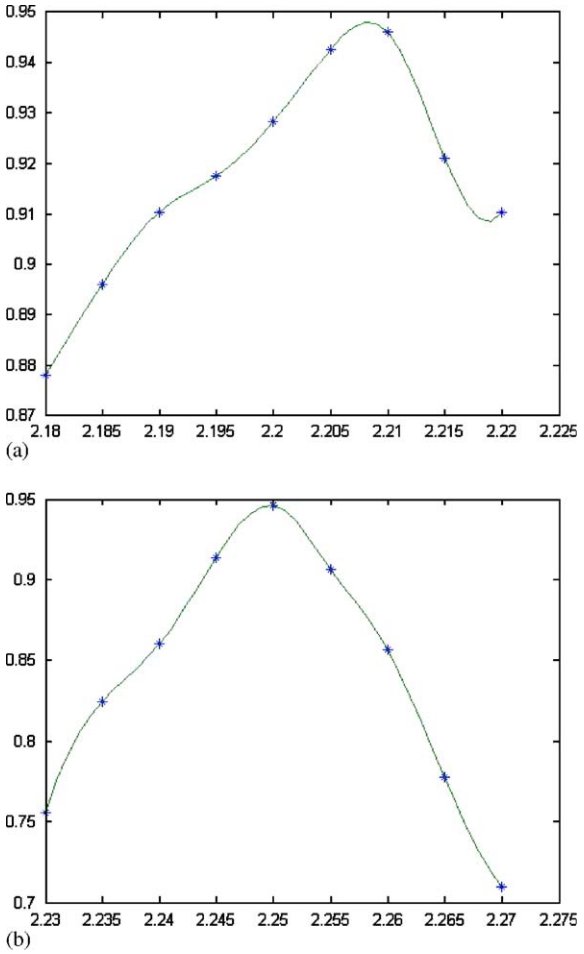

Fig. 5. Correctness versus the derivations of E_I and E_{II}: (a) with E_I and (b) with E_{II}.

6 in category 1, 5 in category 2, 20 in category 3 and 16 in category 4. This is a classification accuracy of approximately 94.61%. Table 3 provides the confusion matrix. It shows that many misclassified irises are to be found in neighboring categories.

To reduce the influence of the border effect on classification accuracy, we have added three iris classification rules. If an iris satisfies one of the rules, it is simultaneously matched in two neighboring categories. As can be seen in Table 4, applying these rules, and with $\Delta E = 0.0050$, the classification was 98.28% accurate. Clearly, this is a great improvement over the method which did not take into account the border effect.

Using coarse iris classification can reduce the time in searching. Table 5 shows the search time with and without coarse iris classification. As shown in Table 5, the search time of our iris recognition system can be reduced to almost 70% of the original search time by using coarse iris classification, if taking into account the border effect, the search time is less than half of the original search time.

Table 3
Classification results of the double threshold algorithm

Assigned category No.	True category No.			
	1	2	3	4
1	48	0	0	6
2	0	321	5	0
3	0	9	175	11
4	0	6	10	281

Table 4
Classification accuracy of the double threshold algorithm with and without border effect

Total samples	Correctly classified samples	Misclassified samples	Classification accuracy (%)
Without border effect	825	47	94.61
With border effect	857	15	98.28

Table 5
The search time of the system with and without coarse classification

Without coarse classification (ms)	Using coarse classification	
	Without border effect (ms)	With border effect (ms)
81	25	32

4.3. Results for the classification using the backpropagation algorithm

In our study using the backpropagation algorithm, 600 iris images randomly selected from the entire collection of 872 iris cases were used as the training data set. The maximal iteration number was set to 600, and three nodes were used in the hidden layer. Fig. 6 illustrates the accuracy of the classification using various training data. The backpropagation algorithm was most accurate when applied to more than 400 samples, but as the number of samples decreased, its accuracy also decreased dramatically. Its best classification result was 93.23% accurate.

4.4. Comparison and discussions

Our results showed that, for two reasons, the double threshold algorithm is a more effective coarse iris classifier than the backprogation algorithm. First, the double threshold

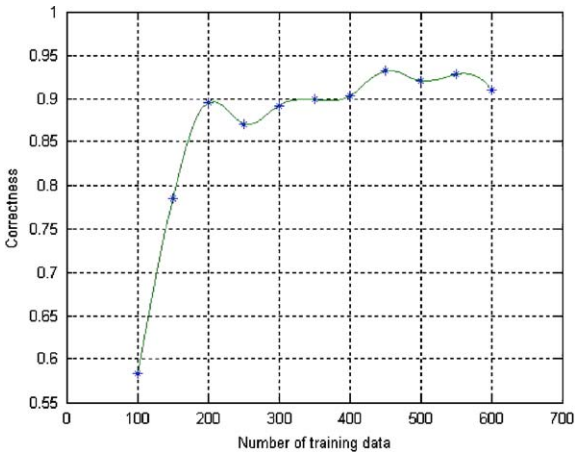

Fig. 6. Classification accuracy of the backpropagation algorithm.

algorithm classifies iris images with an accuracy of 94.61%, against the backprogation algorithm's 93.23%. With this, it should be noted that the classification accuracy of the double threshold algorithm can be greatly increased by taking into account the border effect. Second, the backprogation algorithm takes a long time to train, which is inconsistent with the aim of increasing the system speed.

The results reveal three conditions for misclassification: (1) The texture will be blurry and the calculation of the fractal dimension will be quite unlike its true value if the image resolution is lower than a certain value. (2) The calculation of the fractal dimension will be affected if the eyelids obscure parts of the iris image. (3) It can be difficult to detect textures if an iris image is very dark, it can be difficult to detect textures.

Because of the trade-off between speed and accuracy, the size of the database is a crucial consideration in deciding when to use the coarse classification method. A small database will have short search times and so does not require coarse classification. A recognition system using a large database, however, must consider speed. Iris coarse classification allows the reduction of search times while maintaining high standards of accuracy.

While coarse classification inevitably produces false classifications, it should be noted that the purpose of coarse classification is first to reduce search times. The issue of accuracy is addressed in the following matching step. In this step, a new value is selected as the matching threshold, and the classified image will search for the iris with a matching value smaller than the threshold in its category. If an image is not classified with high confidence at the coarse level, it will be rejected and go to the other categories to match. The detailed measure will combine the recognition method to decide the matching threshold. Further discussion of this, however, is beyond the scope of this paper and will be presented in another future paper.

5. Conclusion

As the demand for information security increases, so does the attention that is paid to biometrics-based, automated personal identification. Among the biometrics approaches, iris recognition is known for its high reliability, but as databases grow ever larger, an approach is needed that can reduce matching times. Iris classification can contribute to that. As the first attempt to classify iris images, this paper presents a novel iris classification algorithm based on the box-counting method of fractal dimension. The approach uses the fractal dimension of the iris image to classify the iris image into four categories according to texture. The classification method has been tested and evaluated on 872 iris cases. This paper discussed in detail not only the selection of thresholds values, but also the influence of the border effect. After taking the border effect into account, the best result was obtained using the double threshold algorithm which was 98.28% accurate.

In future, we will modify the image preprocessing method to reduce the influence of light and eyelids. There is also much work to be done on the selection of classification methods. We will also try other approaches to the improvement of classification accuracy.

Acknowledgements

This work was partially supported by the National Natural Science Foundation of China (NSFC)/High -Tech 863 Fund and The Departmental Fund of the Hong Kong Polytechnic University.

References

[1] A.K. Jain, H. Lin, P. Harath, R. Bolle, An identity-authentication system using fingerprints, Proc. IEEE 85 (9) (1997) 1365–1388.
[2] A.K. Jain, H. Lin, R. Bolle, On-line fingerprint verification, IEEE Trans. Pattern Anal. Mach. Intell. 19 (4) (1997) 302–313.
[3] J.G. Daugman, High confidential visual recognition by test of statistical independence, IEEE Trans. Pattern Anal. Mach. Intell. 15 (11) (1993) 1148–1161.
[4] J.G. Daugman, The importance of being random: statistical principles of iris recognition, Pattern Recognition 36 (2003) 279–291.
[5] R.P. Wildes, Iris recognition: an emerging biometric technology, Proc. IEEE 85 (1997) 1348–1363.
[6] W.W. Boles, B. Boashash, A human identification technique using images of the iris and wavelet transform, IEEE Trans. Signal Process. 46 (4) (1998) 1185–1188.
[7] L. Ma, T. Tan, Y. Wang, D. Zhang, Personal identification based on iris texture analysis, IEEE Trans. Pattern Anal. Mach. Intell. 25 (12) (2003) 1519–1533.
[8] L. Ma, T. Tan, Y. Wang, D. Zhang, Local intensity variation analysis for iris recognition, Pattern Recognition 37 (2004) 1287–1298.

[9] L. Ma, T. Tan, Y. Wang, D. Zhang, Efficient iris recognition by characterizing key local variations, IEEE Trans. Image Process. 13 (6) (2004) 739–749.
[10] B.B. Mandelbrot, J.W. Van Ness, Fractional Brownian motions, fractional noises and applications, SIAM Rev. 10 (4) (1968) 422–437.
[11] A. Pentland, Fractal-based description of natural scenes, IEEE Trans. Pattern Anal. Mach. Intell. 6 (1984) 666–674.
[12] J.M. Keller, S. Chen, R.M. Crownover, Texture description and segmentation through fractal geometry, Comput. Vision Graph Image Process. 45 (1989) 150–166.
[13] B.B. Chaudhuri, N. Sarkar, Texture Segmentation using fractal dimension, IEEE Trans. Pattern Anal. Mach. Intell. 17 (1) (1995) 72–77.
[14] H.O. Peitgen, H. Jurgens, D. Saupe, Chaos and Fractals: New Frontiers of Science, Springer, Berlin, 1992, pp. 202–213
[15] H.O. Peitgen, H. Jurgens, D. Saupe, Chaos and Fractals New Frontiers of Science, Springer, New York, 1992.
[16] R. Rojas, Neural Networks: A Systematic Introduction, Springer, Berlin, 1996, pp. 149–162.
[17] S. Haykin, Neural Networks, second ed., Prentice-Hall, Englewood Cliffs, NJ, 1999, pp. 161–175.
[18] J.A. Anderson, An Introduction to Neural Networks, MIT Press, Cambridge, MA, 1995, pp. 255–277, 454–459.
[19] L. Fu, Neural Networks in Computer Intelligence, McGraw-Hill, New York, 1994, pp. 80–96.

About the Author—LI YU received her B.Sc. degree from the Heilongjiang University in 1998, and her M.Sc. degrees in Øptics from Harbin Institute of Technology (HIT), Harbin, China, in 2000. She is currently a Ph.D. student in the School of Computer Science and Technology at the Harbin Institute of Technology (HIT). Her research interests include pattern recognition, image analysis, and biometrics, etc.

About the Author—DAVID ZHANG graduated in computer science from the Peking University in 1974 and received his M.Sc. and Ph.D. degrees in computer science and engineering from the Harbin Institute of Technology (HIT) in 1983 and 1985, respectively. From 1986 to 1988, he was a postdoctoral fellow at Tsinghua University and became an associate professor at Academia Sinica, Beijing, China. He received his second Ph.D. in electrical and computer engineering at the University of Waterloo, Ontario, Canada, in 1994. Currently, he is a professor in Hong Kong Polytechnic University. He is the Founder and Editor-in-Chief, International Journal of Image and Graphics (IJIG); Book Editor, Kluwer International Series on Biometrics (KISB); and Program Chair, International Conference on Biometrics Authentication (ICBA). He is Associate Editor of more than ten international journals including IEEE Transactions on SMC-A/SMC-C and Pattern Recognition, and is the author of more than 140 journal papers, twenty book chapters and eleven books. As a principal investigator, he has since 1980 brought to fruition many biometrics projects and won numerous prizes. He holds a number of patents in both the USA and China and is a current Croucher Senior Research Fellow.

About the Author—KUANQUAN WANG received his B.E. and M.E. degrees from the Harbin Institute of Technology (HIT), Harbin, China, and his Ph.D. degrees in computer science and technology from Chongqing University, Chongqing, China, in 1985, 1988, and 2001, respectively. From 2000 to 2001 he was a visiting scholar in the Hong Kong Polytechnic University supported by Hong Kong Croucher Funding. From 2003 to 2004 he was a research fellow in the same university. Currently, he is a professor and a supervisor of Ph.D. candidates of the Department of Computer Science and Engineering, and an Associate Director of Biocomputing Research Centre in HIT. So far, he has published over 70 papers. Also he is a member of the IEEE, an editorial board member of International Journal of Image and Graphics. His research interests include biometrics, image processing, and pattern recognition.

About the Author—WEN YANG received the B.Sc. and M.Sc. degrees in Computer Science from the Wuhan University of Science and Technology, China, in 2001 and the Harbin Institute of Technology (HIT), China, in 2004, respectively. His research interests include pattern recognition, biometrics, and cost-based database query optimization.